engineering proceedings

MDPI

Proceeding Paper

Energetic Analysis for the Improvement of a Cupola Furnace †

Axel Vargas Sánchez, Ricardo Galindo Bulos, Juan C. Prince *, Asunción Zárate and Miguel A. Gijón

Tecnologico de Monterrey, Escuela de Ingeniería y Ciencias, Ave. Eugenio Garza Sada 2501, Monterrey 64849, Nuevo León, Mexico; axeleduv26@gmail.com (A.V.S.); a01275545@tec.mx (R.G.B.); azarate@tec.mx (A.Z.); miguel.gijon@tec.mx (M.A.G.)

* Correspondence: jcprince@tec.mx

† Presented at the International Conference on Electronics, Engineering Physics and Earth Science (EEPES 2025), Alexandroupolis, Greece, 18–20 June 2025.

Abstract

Cupola furnaces rank among the oldest melting technologies in steelmaking, relying predominantly on coke as the primary fuel. In this study, a detailed energy analysis was conducted on a cupola unit used for gray and ductile iron production. Energy and thermal analyses were performed on the furnace to improve efficiency and minimize energy losses in the system. Computational simulations with an equation solving program quantified an exhaust-gas heat loss of 1.5 Gigajoules. To recover this waste heat, a heat exchanger was proposed to preheat the incoming combustion air. Numerical simulations of the modified system demonstrate a 3% increase in overall furnace efficiency and a reduction of about ten percent of coke per charge, equivalent to 716 kg per day for the unit under evaluation.

Keywords: cupola furnace; waste heat recovery; heat exchanger; energy efficiency; computational simulation

1. Introduction

The steel production industry plays a crucial role in the global economy and in the manufacturing of diverse industrial products. This industry has undergone significant growth and innovation in steel production methods, with plants and factories dedicated to steel-based manufacturing continuously evolving [1–3]. However, one of the primary manufacturing methods since the mid-19th century remains the cupola furnace, whose invention emerged from the need for a more efficient and low-cost process to melt large quantities of metal, primarily steel, using scrap as the raw material [4,5]. The cupola furnace is a vertical melting vessel that relies on coke combustion to melt raw materials and generate molten metal, which is then poured into sand molds to achieve specific geometries. The aforementioned raw material consists of iron scrap and other metallic elements. During melting, impurities are separated, enabling material reuse [6,7]. The dimensions of these units vary depending on the desired casting quantities. Structurally, they feature a cylindrical shape, with an exterior constructed from steel and an interior lined with refractory materials capable of withstanding the high temperatures inherent to the melting process. A cross-sectional view of its structure and components is provided in Figure 1.

The cupola furnace is divided into three primary zones, each designed to fulfill a specific function, thereby enabling a comprehensive understanding of its integrated operation.

check for updates

Academic Editor: Grigor Mihaylov

Published: 6 September 2025

Citation: Sánchez, A.V.; Bulos, R.G.; Prince, J.C.; Zárate, A.; Gijón, M.A. Energetic Analysis for the Improvement of a Cupola Furnace. *Eng. Proc.* **2025**, *104*, 86. https://doi.org/10.3390/engproc2025104086

Copyright: © 2025 by the authors. Licensee MDPI, Basel, Switzerland. This article is an open access article distributed under the terms and conditions of the Creative Commons Attribution (CC BY) license (https://creativecommons.org/licenses/by/4.0/).

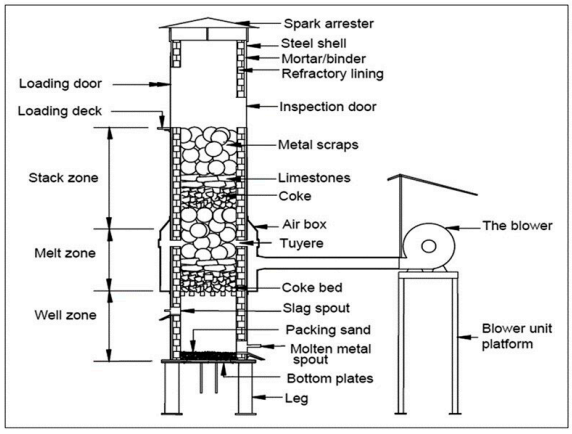


Figure 1. Structural schematic of cupola furnace.

- Charging zone: Located at the uppermost section of the cupola furnace, where raw materials are introduced in the following sequence: coke, metallic scrap, and finally limestone (responsible for impurity separation). This sequential arrangement is critical to ensuring process efficiency.
- Combustion zone: Situated in the middle section, where coke undergoes combustion, generating the heat required to melt the metallic feedstock.
- Well zone: Positioned at the furnace's base, serves as the final stage where molten material settles. Notably, the limestone facilitates slag separation from the molten mixture. Due to density differences, the slag floats atop the molten mixture and is readily separated.

Multiple studies have demonstrated that these three zones can achieve heightened efficiency by optimizing their operational parameters [8–10].

2. Furnace Analysis

After explaining how a cupola furnace works in the previous section, now it is important to identify how the furnace analyzed for this research operates. This will give a clear idea of how the results presented at the end show a clear improvement in the efficiency of the furnace. The cupola furnace used for this research belongs to a company responsible for producing masses and brake drums for heavy-duty vehicles. The material produced in this furnace is gray iron and nodular steel.

Table 1 presents the specific dimensions of the furnace analyzed.

Table 1. Cupola furnace characteristics.

Parameter/Component	Specification
Total height	16.5 m
Internal diameter	0.914 m
Thickness	0.393 m
Charging zone height	5.37 m
Combustion zone height	2.3 m
Well zone height	2.33 m
Construction material	A36 steel plates (1/4″ and 3/16″)

Table 2 shows the characteristics of the air blower that the company is using, presenting important details such as the volumetric flow rate of the air entering the furnace during the combustion stage.

Table 2. Air blower characteristics.

Air Blower	Specification
Brand	Chicago Blower
Model	D53/I3/BH/CW
Volumetric flow rate	1.085 m^3/s
Rotational speed	3859 rpm *

* rpm: revolutions per minute.

For the production of gray iron and nodular steel, this furnace operates with the metal charge, coke, and limestone (ls) quantities detailed in Table 3. The operating parameters of the furnace are summarized in Table 4.

Table 3. Charge materials and quantities.

Charge Material	Quantity per Charge (kg)
Metal scrap	220
Coke	34
Limestone (ls)	12

Table 4. Operating parameters.

Parameter	Gray Iron	Nodular Steel
Metal melting time between taps	First tap: 28–32 min Post-first tap interval: 8–16 min	First tap: 28–32 min Post-first tap interval: 8–16 min
Charges per shift	160–198	90–110

3. Development and Analysis of Model

3.1. Mass Balance Analysis

The analysis initiates with a mass balance, M, in Equation (1), where the system is assumed to operate under steady-state flow conditions. This yields (2), which represents the sum of mass inputs and outputs:

$$M_{in} - M_{out} = \Delta M_{furnace} \quad (1)$$

$$\Sigma M_{in} = \Sigma M_{out} \quad (2)$$

The principle of mass conservation is applied to a generalized mass balance equation encompassing the total mass of materials within the smelting process, as formulated in (3), where M_{fg} denotes the mass of flue gas, the residual gases generated during the combustion process. Figure 2 provides a schematic representation of the relationship described by the following equation:

$$M_{coke} + M_{air} + M_{metal} + M_{ls} = M_{metal,out} + M_{slag} + M_{fg} \quad (3)$$

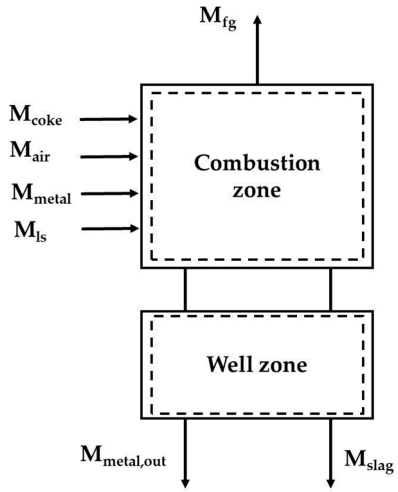


Figure 2. Mass transfer in cupola furnace.

3.2. Energy Balance Analysis

Regarding the energy transfer in the form of heat within the system, an energy balance is carried out as given by (4), indicating that the sum of the incoming heat is equal to the sum of the outgoing heat:

$$\Sigma Q_{in,i} = \Sigma Q_{out,i} \tag{4}$$

The combustion zone is analyzed in Figure 3, which is one of the three zones mentioned earlier. It is divided into the combustion section (A) and the melting section (B). The heat entering and exiting each part is indicated, followed by a detailed analysis of the heat exchanges.

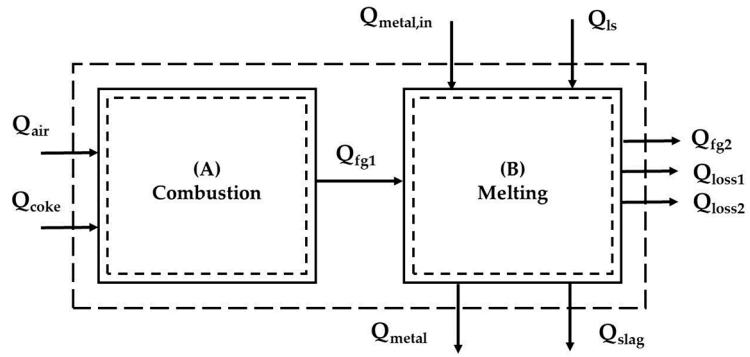


Figure 3. Heat transfer in cupola furnace.

3.2.1. Heat Transfer in Combustion Zone (A)

Heat input is assumed to occur through an adiabatic process, which integrates the sum of the heat input from both the fuel and the air, shown by (5), where Q_{fg} denotes the heat of the flue gas:

$$Q_{fg1} = Q_{coke} + Q_{air} \tag{5}$$

The heat of both coke and air is calculated via Equations (6)–(9), which account for their respective mass (M), specific heat at constant volume (C_v), specific heat at constant pressure (C_p), and temperature (T):

$$Q_{coke} = M_{coke} C_{v\,coke} \tag{6}$$

$$Q_{air} = Q_{O2,in} + Q_{N2,in} \tag{7}$$

$$Q_{O2,in} = M_{O2,in} C_{p\,O2,in} T_{aire,in} \tag{8}$$

$$Q_{N2,in} = M_{N2,in} C_{p\,N2,in} T_{aire,in} \quad (9)$$

3.2.2. Heat Transfer in Melting Zone (B)

Since Equation (5) is used to determine the heat input to the melting zone, Equation (10) is used to define the heat outputs occurring in this zone.

$$Q_{out} = Q_{metal} + Q_{slag} + Q_{fg2} + Q_{loss1} + Q_{loss2} \quad (10)$$

where Q_{metal} is the heat involved in melting the metal (heat in the stock), Q_{slag} is the heat content of the slag formed, Q_{fg2} is the heat content of the fuel gas exiting the flue, Q_{loss1} is the heat loss through the walls of the combustion zone, and Q_{loss2} refers to the heat loss through the walls of the stack zone. Therefore, the total heat input and output in the combustion zone represented in Figure 3 can be expressed using (11):

$$Q_{coke} + Q_{air} = Q_{metal} + Q_{slag} + Q_{fg2} + Q_{loss1} + Q_{loss2} \quad (11)$$

3.2.3. Metal Melting

The heat required to melt the metal is obtained by adding the sensible heat ($Q_{s,metal}$) and the latent heat ($Q_{l,metal}$) present in this phase change from solid to liquid, as shown in (12).

$$Q_{metal} = Q_{s,metal} + Q_{l,metal} \quad (12)$$

Sensible heat, which refers to the energy supplied to increase from the initial temperature to the melting point, is defined by (13), which takes into account the mass (M_{metal}), the specific heat at constant pressure ($C_{p_{metal}}$), and both the initial ($T_{metal,in}$) and melting ($T_{metal,mt}$) temperatures.

$$Q_{s,metal} = M_{metal} C_{p_{metal}} (T_{metal,mt} - T_{metal,in}) \quad (13)$$

Latent heat, which is the energy required to change the phase (in this case from solid to liquid), is defined by (14), where $Q_{lf,metal}$ represents the latent heat of melting the metal.

$$Q_{l,metal} = M_{metal} Q_{lf,metal} \quad (14)$$

3.2.4. Heat in Slag

In the case of slag, it works according to (15), where the heat from the limestone and the heat from the accumulated ash are added.

$$Q_{slag} = Q_{ls} + Q_{ash} \quad (15)$$

As with metal, the heat required to burn limestone involves sensible heat and latent heat, as shown in (16), where $Q_{s,ls}$ is the sensible heat and $Q_{l,ls}$ is the latent heat.

$$Q_{ls} = Q_{s,ls} + Q_{l,ls} \quad (16)$$

Both heats, $Q_{s,ls}$ and $Q_{l,ls}$, are given by Equations (17) and (18), whose variables are described prior to (13).

$$Q_{s,ls} = M_{ls} C_{p_{ls}} (T_{ls,mt} - T_{ls,in}) \quad (17)$$

$$Q_{l,ls} = M_{ls}\, Q_{lf,ls} \quad (18)$$

In the case of ash, the heat is similar to the latent heat of limestone and metal, as described in (19).

$$Q_{ash} = M_{ash} C_{p_{ash}} \left(T_{slag} - T_{coke,in} \right) \tag{19}$$

3.2.5. Heat in Exhaust Gases

The total heat of the exhaust gases $\left(Q_{fg2} \right)$ is given by the sum of the heats of each of the gases resulting from combustion, as shown in (20). The gases present are carbon dioxide, water vapor, sulfur dioxide, oxygen, and nitrogen.

$$Q_{fg2} = Q_{CO2} + Q_{H2O} + Q_{SO2} + Q_{O2,out} + Q_{N2,out} \tag{20}$$

$$Q_{CO2} = M_{CO2} C_{p_{CO2}} \left(T_{fg2} - T_{coke,in} \right) \tag{21}$$

$$Q_{H2O} = M_{H2O} C_{p_{H2O}} \left(T_{fg2} - T_{coke,in} \right) \tag{22}$$

$$Q_{SO2} = M_{SO2} C_{p_{SO2}} \left(T_{fg2} - T_{coke,in} \right) \tag{23}$$

$$Q_{O2,out} = M_{O2,out} C_{p_{O2,\ out}} \left(T_{fg2} - T_{coke,in} \right) \tag{24}$$

$$Q_{N2,out} = M_{N2,out} C_{p_{N2,\ out}} \left(T_{fg2} - T_{coke,in} \right) \tag{25}$$

where M_{CO2}, M_{H2O}, $M_{O2,out}$, and $M_{N2,out}$ are the masses of CO_2, H_2O, SO_2, O_2, and N_2 in the flue gas; and $C_{p_{CO2}}$,$C_{p_{H2O}}$,$C_{p_{SO2}}$,$C_{p_{O2,out}}$, and $C_{p_{N2,out}}$ represent the specific heat capacities of CO_2, H_2O, SO_2, O_2, and N_2 in the flue gas at outlet temperature, while T_{fg2} denotes the gas outlet temperature of the furnace.

3.2.6. Heat Losses Through Walls

The heat loss through the furnace walls in the two zones following the charging operation is calculated. First, the heat loss in the combustion zone is determined via Equation (26), where the heat transfer rate is multiplied by the operating time t per charge:

$$Q_{loss1} = q_{loss1} * t \tag{26}$$

This heat transfer rate is calculated via (27), which accounts for the ambient temperature (T_a), the internal furnace temperature $\left(T_{f,ad} \right)$, and the total thermal resistance (R_{th-tot}):

$$q_{loss1} = \frac{T_{f,ad} - T_a}{R_{th-tot}} \tag{27}$$

The total thermal resistance is determined by the three heat transfer mechanisms—radiation, conduction, and convection—as expressed in (28):

$$R_{th-tot} = R_{th-rad} + R_{th-cond} + R_{th-conv} \tag{28}$$

The missing data were calculated and analyzed using their respective formulas. For the radiative thermal resistance, the radiative heat transfer coefficient, wall material emissivity, Stefan–Boltzmann constant, heat transfer surface area, and internal wall temperature in this zone were determined. The conductive thermal resistance was derived by applying Fourier's law to cylindrical surfaces. Thermal conductivity constants of the wall materials and their sectional thicknesses were identified. Regarding convective thermal resistance, a formula correlating the heat transfer surface with the convective heat transfer coefficient was employed. The latter requires an extended procedure, as it involves dimensionless parameters such as the Nusselt, Rayleigh, Grashof, and Prandtl numbers.

Subsequently, the heat loss in the well zone was calculated. The procedure applied to the previous zone was repeated, with variables adjusted to account for distinct zonal conditions. Equations (29)–(31) describe this adapted process, incorporating new variables due to these changes:

$$Q_{loss2} = q_{loss2} * t \tag{29}$$

$$q_{loss2} = \frac{T_{fg2} - T_a}{R_{th-tot2}} \tag{30}$$

$$R_{th-tot2} = R_{th-rad2} + R_{th-cond2} + R_{th-conv2} \tag{31}$$

3.2.7. Heat Transfer in Well Zone

The well zone is where molten material settles and is discharged into designated containers for both the final metal product (iron/steel) and slag. Figure 4 illustrates the heat input from the molten metal and slag streams, as well as heat losses through the furnace walls and via the outgoing slag and metal. These conclusions are derived from an energy balance analysis, as formulated in (32), which accounts for thermal interactions across the system boundaries:

$$Q_{metal} + Q_{slag,in} = Q_{metal,out} + Q_{slag,out} + Q_{loss3} \tag{32}$$

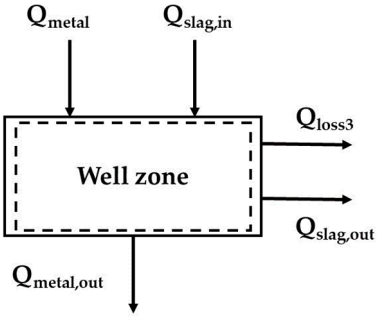


Figure 4. Heat transfer in well zone.

It is assumed that the slag's heat remains constant between the inlet and outlet, enabling its exclusion from the energy balance. The outcome of this simplification is formulated in (33).

$$Q_{metal} = Q_{loss3} + Q_{metal,out} \tag{33}$$

where Q_{loss3}, the unknown heat loss through the furnace walls in this zone, is isolated and expressed as follows:

$$Q_{loss3} = Q_{metal} - Q_{metal,out} \tag{34}$$

The heat output of the metal is calculated by summing its sensible $(Q_{s,metal2})$ and latent heat $(Q_{l,m})$:

$$Q_{metal,out} = Q_{s,metal2} + Q_{l,m} \tag{35}$$

A new variable, $Q_{s,metal2}$, is introduced to represent the sensible heat of the outgoing metal after undergoing heat loss in the well zone. This relationship is expressed in (36), where the casting temperature, $T_{metal,tp}$, is employed to quantify the thermal state of the metal prior to discharge:

$$Q_{s,metal2} = M_{metal} C_{p_{metal}} \left(T_{metal,tp} - T_{metal,in} \right) \tag{36}$$

3.3. Furnace Efficiency

The furnace efficiency is determined to be the ratio of heat effectively utilized in the melting process to the total heat supplied via the combustion of coke and air. Alternatively, efficiency can be calculated based on heat losses incurred during the process. For the analyzed furnace, the first approach was employed, utilizing (37).

$$\eta_{\text{furnace}} = \frac{Q_{metal,out}}{Q_{fg1}} \tag{37}$$

4. Technical Improvement Proposal

Studies such as that by Norwood et al. [11] indicate that implementing a heat recovery system can minimize fuel consumption and enhance the efficiency of cupola furnaces. Following an analysis of the furnace performance in this study, significant heat losses were identified, primarily in the flue gases $\left(Q_{fg2}\right)$. Consequently, it was proposed that this waste heat could be harnessed to improve thermal efficiency. To optimize the combustion process efficiency, the installation of a finned-tube heat exchanger is recommended. As reported by [12], this technology maximizes the utilization of heat contained in combustion gases, which are currently wasted through high-temperature atmospheric discharge.

The proposed system involves a heat exchanger in which hot flue gases from the furnace flow through the inner tubes, while combustion air—requiring preheating—circulates externally across the finned surfaces. The incorporation of fins significantly increases the heat transfer area, thereby enhancing thermal efficiency. Furthermore, finned-tube heat exchangers exhibit robustness under high-temperature conditions and are suitable for handling dust-laden or particulate-containing gases, such as those generated during coke combustion.

Performance analysis of the furnace with the proposed heat exchanger was conducted using Equations (38)–(40). Here, $Q_{reg,real}$ denotes the current heat available without the heat exchanger as combustion air enters the system, while $Q_{reg,ideal}$ represents the ideal regenerable heat achievable via the heat exchanger. The dimensionless heat transfer effectiveness, ε, is defined by (40).

$$Q_{reg,real} = M_{air} c_{p_{air}} (T_{s,cold\ air} - T_{in}) \tag{38}$$

$$Q_{reg,ideal} = M_{air} c_{p_{air}} \left(T_{fg2} - T_{in}\right) \tag{39}$$

$$\varepsilon = \frac{Q_{reg,real}}{Q_{reg,ideal}} \tag{40}$$

The results, summarized in Table 5, demonstrate that $Q_{reg,ideal}$ is twice the $Q_{reg,real}$, highlighting the potential for enhanced thermal efficiency through optimized heat recovery.

Table 5. Regenerated heat.

Parameter	kW
$Q_{reg,real}$	314
$Q_{reg,ideal}$	684
ε	0.458 (45.8%)

The effectiveness–NTU method is employed to establish the performance requirements that the heat exchanger must meet in order to operate at maximum efficiency. The dimensionless number of transfer units (NTU), defined in (41), quantifies the exchanger's capacity to transfer heat; in this expression, U is the overall heat transfer coefficient; A is

the total heat transfer surface area; and C_{min} denotes the smaller heat-capacity rates of the two working fluids.

$$\text{NTU} = \frac{U * A}{c_{min}} \tag{41}$$

$$C = M * c_p \tag{42}$$

First of all, it is important to emphasize the calculation of the overall heat transfer coefficient (U) given from (43), where h_1 is the air heat transfer coefficient and h_2 is the flue gases heat transfer coefficient, both given by (44) and (45):

$$\text{U} = \frac{\frac{1}{\frac{1}{h_1}+\frac{1}{h_2}}}{1000} \tag{43}$$

$$h_1 = Nu_{Air} * \frac{k_{Air}}{D_{tube}} \tag{44}$$

$$h_2 = Nu_{Gas} * \frac{k_{Gas}}{D_{Gas}} \tag{45}$$

Nu_{Air} and Nu_{Gas} are the Nusselt numbers of both fluids, k_{Air} and k_{Gas} are the thermal conductivity of both fluids, D_{tube} is the diameter of the tube through which the air will pass, and D_{Gas} refers to the dimension of the space through which the flue gases will pass. The Nusselt numbers are given by (46) and (47), where it is necessary to use the Reynolds numbers (Re_{Air} y Re_{Gas}) and the Prandtl number (Pr_{Air} y Pr_{Gas}) for both equations.

$$Nu_{Air} = 0.023 * \left({Re_{Air}}^{0.8} * {Pr_{Air}}^{0.4} \right) \tag{46}$$

$$Nu_{Gas} = 0.023 * \left({Re_{Gas}}^{0.8} * {Pr_{Gas}}^{0.4} \right) \tag{47}$$

It is important to remember that the Reynolds numbers are given for air by (48) and for flue gases by (49), both of which use the variables (Air_{speed}) (50) and (Gas_{speed}), whose values are given by the company that owns the furnace. Last but not least, the Reynolds numbers also use μ_{Air} and μ_{Gas}, which represent the kinematic viscosity of the fluid.

$$Re_{Air} = \frac{Air_{speed} * D_{tube}}{\mu_{Air}} \tag{48}$$

$$Re_{Gas} = \frac{Gas_{speed} * D_{Gas}}{\mu_{Gas}} \tag{49}$$

$$Air_{speed} = \frac{Tube_{flow}}{Tube_{area}} \tag{50}$$

$Tube_{flow}$ and $Tube_{area}$ are given by (51) and (52), respectively; $Tube_{VolFlow}$ refers to the volumetric flow rate per tube.

$$Tube_{flow} = \frac{Tube_{VolFlow}}{28} \tag{51}$$

$$Tube_{area} = \pi {R_{in}}^2 \tag{52}$$

$$Tube_{VolFlow} = \frac{2300 * 0.283}{60} \tag{53}$$

The heat-capacity rates of both fluids were calculated, revealing that the exchanger's minimum heat-capacity rate, C_{min}, corresponds to the cold fluid (air) with a value of 1477 kW/K, whereas the maximum heat-capacity rate, C_{max}, corresponds to the hot fluid (combustion gases) with a value of 1938 kW/K. These values were then applied to the NTU–

effectiveness chart shown in Figure 5 [6,13]; by correlating the exchanger's effectiveness with the ratio C_{min}/C_{max}, an NTU of 0.8 is obtained. Finally, the required heat transfer surface area, A, is determined by rearranging (54).

$$A = \frac{C_{min} * NTU}{U} \quad (54)$$

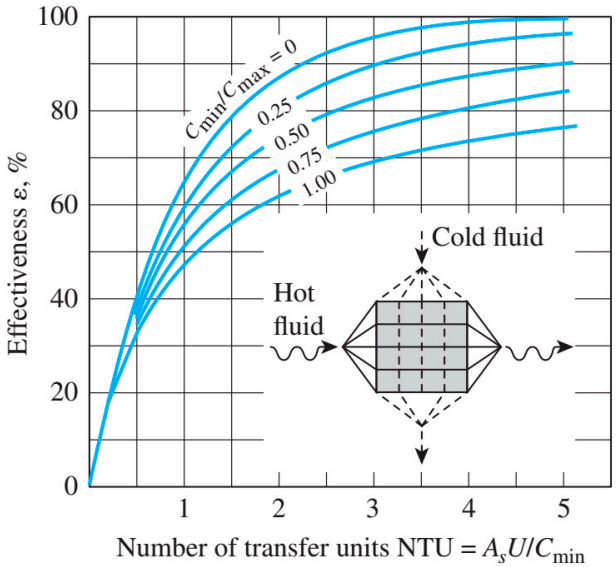


Figure 5. Effectiveness–NTU curve for cross-flow heat exchanger with unmixed fluid streams.

A total heat exchange surface area of 68.97 m^2 was determined. For a 3-inch-diameter tube geometry, this corresponds to a cumulative tube length of 43.02 m, which is arranged as 28 tubes, each 1.57 m long. A total of 8232 heat transfer fins are incorporated (equivalent to 294 fins per tube). Under this configuration, and based on simulations conducted with the Engineering Equation Solver (EES) [14], the furnace's thermal efficiency increases by 3%, reflecting the recovery of heat that would otherwise be lost in the exhaust gases. Consequently, the required coke charge can be reduced due to the elevated temperature of the inlet air stream (formerly at ambient temperature).

This improvement translates into a significant fuel saving, as detailed in Table 6, which contrasts furnace performance with and without the heat exchanger.

Table 6. Furnace performance comparison.

Parameter	Without Heat Exchanger	With Heat Exchanger
Thermal efficiency, η	0.21	0.24
Coke mass per charge (kg)	34	30
Fuel energy requirement (coke) (MJ) *	4457	3932

* MJ: megajoules.

A reduction of 4 kg of coke per charge is observed. Taking into account the data in Table 4, which shows an average of 179 charges per shift, along with the fact that the furnace operates three shifts per day and the current market price of coke (0.162 USD kg^{-1}), the resulting cost savings are summarized in Table 7.

Table 7. Estimated savings from reduced coke consumption.

Period	Coke Savings (kg)	Cost Savings (USD)
Shift	716	115.99
Day	2148	347.97
Week	10,740	1739.88
Month	64,440	10,439.28
Year	773,280	125,271.36

5. Conclusions

A comprehensive mass balance of a cupola furnace was first performed, followed by a stage-by-stage energy analysis, from the combustion zone to the well section, quantifying the heat flows involved. Employing heat transfer principles, we then evaluated the process's thermal losses and identified substantial heat discharge via the exhaust gases. To recover this otherwise wasted energy, a finned-tube heat exchanger was proposed to preheat the combustion air stream, thereby enhancing furnace thermal efficiency and reducing coke consumption. The design of the exchanger leveraged the effectiveness–NTU method to determine the optimal geometry for maximum heat transfer, yielding a layout of 28 tubes fitted with a total of 8,232 fins. Although installation of the exchanger incurs an initial capital outlay, the projected long-term fuel savings render the investment highly advantageous.

Author Contributions: Conceptualization, J.C.P.; Methodology, J.C.P., A.Z. and M.A.G.; Validation, A.V.S. and R.G.B.; Formal Analysis, A.Z. and M.A.G.; Investigation, A.V.S. and R.G.B.; Writing—Original Draft, A.V.S. and R.G.B.; Writing—Review and Editing, J.C.P.; Visualization, A.V.S., R.G.B., J.C.P., A.Z. and M.A.G. All authors have read and agreed to the published version of the manuscript.

Funding: This research received no external funding.

Institutional Review Board Statement: Not applicable.

Informed Consent Statement: Not applicable.

Data Availability Statement: No new data were created.

Acknowledgments: The authors acknowledge the support provided by Tecnológico de Monterrey, Mexico.

Conflicts of Interest: The authors declare no conflicts of interest.

References

1. Pribulova, A.; Baricova, D.; Futas, P.; Pokusova, M.; Eperjesi, S. Cupola furnace slag: Its origin, properties and utilization. *Int. J. Met.* **2019**, *13*, 627–640. [CrossRef]
2. Raja, R.; Kumar, S. Cupola slag as a green concrete-making material and its performance characteristics-A review. *Renew. Sustain. Energy Rev.* **2023**, *185*, 113573. [CrossRef]
3. Ochejah, Y.Y.; Cyril, O.; Omaone, I.F.; Ogwudubi, A.F.; Onakemu, O.A. Cupola Furnace Design and Fabrication for Industrial Development. *Int. J. Sci. Adv.* **2021**, *2*, 102–106. [CrossRef]
4. Jardón, L.E.; (Universidad Nacional Autónoma de México, Mexico City, Mexico). Lecture Notes: Introduction to Metallurgical and Materials Process Engineerings, 2020.
5. Meredith, J. The Cupola Furnace. Atlas Foundry Company Publications. Available online: http://www.atlasfdry.com/cupolafurnace.htm (accessed on 24 April 2025).
6. Raymond, H.M. Modern Shop Practice, Part 1–3. Available online: https://upload.wikimedia.org/wikipedia/commons/b/b1/Modern_shop_practice%3B_a_general_reference_work_-_Vol._2_%28IA_modernshoppracti02unse%29.pdf (accessed on 24 April 2025).
7. Niehoff, T.; Struning, H.; Lemperle, M. Oxy-fuel burner technology for cupola melting. In Proceedings of the 2nd International Cupola Conference, Trier, Germany, 18–19 March 2004.

8. Ajah, S.A.; Idorenyin, D.; Ezurike, B.O.; Nwokenkwo, U.; Ikwuagwu, C.V. Thermal analysis to investigate the effects of operating parameters on conventional cupola furnace efficiency. *Proc. Inst. Mech. Eng. Part E J. Process Mech. Eng.* **2023**, *237*, 1354–1366. [CrossRef]
9. Sultanguzin, I.A.; Isaev, M.V.; Kurzanov, S.Y. Optimizing the production of coke, coal chemicals, and steel on the basis of environmental and energy criteria. *Metallurgist* **2011**, *54*, 600–607. [CrossRef]
10. Rathod, K.; Gupta, S.; Sharma, A.; Prakash, S. Energy-efficient melting technologies in foundry industry. *Indian Foundry J.* **2016**, *62*, 39–46.
11. Norwood, C.; Noble, A.; Williams, S. *Iron Melting Cupola Furnace with Heat Recuperating System (MSE/ME 499 Project)*; University of Alabama: Birmingham, UK, 2010; pp. 1–91.
12. Basavarajappa, S.; Manavendra, G.; Prakash, S.B. A review on performance study of finned tube heat exchanger. *Int. J. Heat Mass Transf.* **2023**, *180*, 121789. [CrossRef]
13. Çengel, Y.A.; Ghajar, A.J. *Heat and Mass Transfer: Fundamentals and Applications*, 5th ed.; McGraw-Hill Education: Columbus, OH, USA, 2015.
14. Klein, S.A. EES—Engineering Equation Solver, Version 12.068. F-Chart Software. Available online: https://fchartsoftware.com (accessed on 24 April 2025).

Disclaimer/Publisher's Note: The statements, opinions and data contained in all publications are solely those of the individual author(s) and contributor(s) and not of MDPI and/or the editor(s). MDPI and/or the editor(s) disclaim responsibility for any injury to people or property resulting from any ideas, methods, instructions or products referred to in the content.